

Energy Expressions and Free Vibration Analysis of A Rotating Uniform Timoshenko Beam Featuring Bending-Torsion Coupling

Metin O. Kaya* and Ozge Ozdemir Ozgumus

Istanbul Technical University, Faculty of Aeronautics and Astronautics, 34469, Maslak,
Istanbul, Turkey

Abstract

In this study; free vibration analysis of a uniform, rotating, cantilever Timoshenko beam featuring coupling between flapwise bending and torsional vibrations is performed. At the beginning of the study, kinetic and potential energy expressions of a rotating Timoshenko beam having single cross-sectional symmetry are derived by using several explanatory tables and figures. In the following section, Hamilton's principle is applied to the derived energy expressions to obtain the governing differential equations of motion. The parameters for the hub radius, rotational speed, rotary inertia, shear deformation, slenderness ratio and bending-torsion coupling are incorporated into the equations of motion. In the solution part, an efficient mathematical technique, called the Differential Transform Method (DTM), is used to solve the governing differential equations of motion. Using the computer package, Mathematica, the mode shapes are plotted, the effects of the incorporated parameters on the natural frequencies are investigated. The calculated results are tabulated in several tables and plotted in several graphics. In order to validate the calculated results, the beam is also modeled in the finite element program, ABAQUS. Moreover, two illustrative examples, chosen from open literature, are solved for further validation. Consequently, it is observed that there is a good agreement between the results.

* *Corresponding Author*: Tel: +90 212 2853110, Fax: +90 212 2852926
E-mail: kayam@itu.edu.tr (M.O.Kaya)

Keywords: Rotating coupled Timoshenko beam, bending-torsion coupling, Differential Transform Method, Differential Transformation

1. Introduction

When the cross-sections of an isotropic beam have two symmetric axes, the shear center and the centroid of the cross-sections coincide. Therefore, transverse and lateral bending vibrations are not coupled with the torsional vibration. However, when the cross-sections have only one symmetry axis, the shear center and the centroid do not coincide and the bending vibration that occurs in the plane perpendicular to the symmetry axis is coupled with the torsional vibration.

Several engineering components, such as blades in turbines, compressors, propellers or helicopter rotors, usually have non-coincident elastic and inertial axes, which are respectively the shear centers and the loci of centroids of the cross-sections. Therefore, the determination of the dynamic characteristics of rotating coupled beams is of great importance in the design of such components. As a result, free and forced vibration characteristics of bending-torsion coupled beams have been an interesting area for many researchers. Houbolt and Brooks (1958) derived the equations of motion of a cantilever Euler-Bernoulli beam in coupled bending-bending-torsion vibration motion by including the rotation effects. Bishop and Price (1977) studied the coupled bending-torsion vibration of the Timoshenko beams without including the warping stiffness. Subrahmanyam et. al. (1981) presented natural frequencies and modal shapes of a rotating blade of asymmetrical aerofoil cross-section with allowance for shear deflection and rotary inertia. Hallauer and Liu (1982) derived the exact dynamic stiffness matrix for a bending-torsion coupled Euler-Bernoulli beam with the warping stiffness ignored.

Dokumaci (1987) derived the exact analytical expressions for the solution of the bending–torsion equations without the warping effect. Bishop et. al. (1989) extended the study of Dokumaci by including the warping effect. Banerjee and Williams (1992, 1994) derived the analytical expressions for the coupled bending–torsion dynamic stiffness matrix of a Timoshenko beam excluding the warping stiffness effect. Banerjee et. al. (1996) recast the study of Bishop et. al. (1989) by using the dynamic stiffness matrix. Eslimy-Isfahany et. al. (1996) studied the response of a bending-torsion coupled beam to deterministic and random loads. Bercin and Tanaka (1997) included the effects of warping, shear deformation and rotary inertia in their study of coupled flexural-torsional vibrations of beams having single axis of symmetry. Hashemi and Richard (2000) presented a new dynamic finite element for the bending–torsion coupled Euler-Bernoulli beams with the warping stiffness omitted. Sabuncu and Evran (2005) studied the dynamic stability of an asymmetric cross-section rotating Timoshenko beam without pretwist.

In this study, which is an extension of the authors' previous works [Kaya (2006), Özdemir and Kaya (2006a), Ozdemir Ozgumus and Kaya (2006b)], free vibration analysis of a uniform, rotating, cantilever Timoshenko beam featuring coupling between flapwise bending and torsional vibrations is performed. At the beginning of this study both the kinetic and the potential energy expressions are derived step by step using explanatory tables and figures. The parameters for the hub radius, rotational speed, rotary inertia, shear deformation, slenderness ratio and bending-torsion coupling are incorporated into the formulation. Furthermore, the governing differential equations of motion and the related boundary conditions are obtained applying the Hamilton's principle to the derived energy expressions and solved using an efficient mathematical

technique, called the Differential Transform Method (DTM). Using the computer package, Mathematica, the natural frequencies are calculated, the mode shapes are plotted and the effects of the incorporated parameters are investigated. Unfortunately, a suitable example was not present in open literature for validation. Therefore, the examined beam is modeled in the finite element program, ABAQUS in order to validate the calculated results of this study. Additionally, two examples that study simpler Timoshenko beam models are found in open literature and solved in order to make comparisons. Consequently, it is observed that there is a good agreement between the results.

Partial differential equations are often used to describe engineering problems whose closed form solutions are very difficult to establish in many cases. Therefore, approximate numerical methods, i.e. finite element, finite difference, boundary element methods, etc. are often preferred. However, in spite of the advantages of these on hand methods and the computer codes that are based on them, closed form solutions are more attractive due to their implementation of the physics of the problem and their convenience for parametric studies. Moreover, closed form solutions have the capability and facility to solve inverse problem of determining and designing the geometry and characteristics of an engineering system and to achieve a prescribed behaviour of the system. Considering the advantages of the closed form solutions mentioned above, the Differential Transform Method, DTM, is introduced in this study as the solution method. In open literature, there are several studies that used DTM to deal with linear and nonlinear initial value problems, eigenvalue problems, ordinary and partial differential equations, aeroelasticity problems, etc. A brief review of these studies is given by Ozdemir Ozgumus and Kaya (2006b).

2. Beam Configuration

The governing differential equations of motion are derived for the bending-torsion coupled free vibration of a rotating, uniform, cantilever Timoshenko beam represented by Figure 1, in a right-handed Cartesian coordinate system. Here, the xyz axes constitute a global orthogonal coordinate system with origin at the root of the beam. The x -axis coincides with the neutral axis of the beam in the undeflected position, the z -axis is parallel to the axis of rotation, but not coincident and the y -axis lies in the plane of rotation.

FIGURE 1

Here, a uniform cantilever beam of length L , height h and width b which is fixed at point O to a rigid hub with radius R , is shown. The hub is assumed to be rotating in the counter-clockwise direction at a constant angular velocity, Ω .

The cross-sectional view and the associated dimensions are introduced in Figure 2. As it is seen in Figure 2, the cross-section of the beam is symmetric only about one axis which is the y axis. Therefore, as mentioned in the introduction part the mass and elastic axes of the beam, which are respectively the loci of centroids and shear centers of the cross-sections, are separated by a distance e , as shown in Figure 1 and the flapwise bending vibration is coupled with the torsional vibration.

FIGURE 2

The following assumptions are made in this study,

- a. The flapwise bending displacement is small.
- b. The planar cross sections that are initially perpendicular to the neutral axis of the beam remain plane, but no longer perpendicular to the neutral axis during bending.

c. The beam material is homogeneous and isotropic.

3. Derivation of the Equations of Motion

Derivations of both the kinetic and potential energy expressions are made by considering Figures 3(a) and 3(b) where the cross-sectional and the side views of the flapwise bending-torsion coupled motion of a rotating, uniform Timoshenko beam are given. In this study, coupling that occurs between flapwise bending and torsion is examined. Since the chordwise bending vibration is not included, it is not considered in any figure or formula.

FIGURES 3(a) and 3(b)

Here, a reference point is chosen and is represented by P_0 before deformation and by P after deformation.

3.1. Derivation of the Potential Energy Expression

Considering Figures 3(a) and 3(b), the coordinates of the reference point are given as follows

a. Before deformation (coordinates of P_0):

$$x_0 = R + x \quad (1a)$$

$$y_0 = \eta \quad (1b)$$

$$z_0 = \xi \quad (1c)$$

b. After deformation (coordinates of P):

$$x_1 = R + x + u_0 - (\xi \cos \psi + \eta \sin \psi) \sin \varphi \quad (2a)$$

$$y_1 = \eta \cos \psi - \xi \sin \psi \quad (2b)$$

$$z_1 = w + \xi \cos \psi + \eta \sin \psi \quad (2c)$$

where x is spanwise coordinate, u_0 is the axial displacement due to the centrifugal force, η and ξ are the sectional coordinates of P_0 , w is the flapwise bending displacement, φ is the rotation angle due to bending, γ is the shear angle and ψ is the torsion angle.

The rotation angle due to bending, φ and the torsion angle ψ are small so it is assumed that $\sin \varphi \cong \varphi$ and $\sin \psi \cong \psi$. However, in order to investigate the torsional stability, the second order term of the series expansion of $\cos \psi$ is kept so it is assumed that $\cos \psi \cong 1 - \frac{\psi^2}{2}$ [Hodges and Dowell (1974), Houbolt and Brooks (1957)]. Using these assumptions, equations (2a)-(2c) are rewritten as follows

$$x_1 = R + x + u_0 - \left[\xi \left(1 - \frac{\psi^2}{2}\right) + \eta \psi \right] \varphi \quad (3a)$$

$$y_1 = \eta \left(1 - \frac{\psi^2}{2}\right) - \xi \psi \quad (3b)$$

$$z_1 = w + \xi \left(1 - \frac{\psi^2}{2}\right) + \eta \psi \quad (3c)$$

Knowing that \vec{r}_0 and \vec{r}_1 are the position vectors of the reference point before and after deformation respectively, the position vector differentials can be given by

$$d\vec{r}_0 = (dx_0)\vec{i} + (dy_0)\vec{j} + (dz_0)\vec{k} \quad (4a)$$

$$d\vec{r}_1 = (dx_1)\vec{i} + (dy_1)\vec{j} + (dz_1)\vec{k} \quad (4b)$$

where \vec{i} , \vec{j} and \vec{k} are the unit vectors in the x , y and z directions, respectively.

The components of $d\vec{r}_0$ and $d\vec{r}_1$ are expressed as follows

$$dx_0 = dx \quad (5a)$$

$$dy_0 = d\eta \quad (5b)$$

$$dz_0 = d\xi \quad (5c)$$

$$dx_1 = \left\{ 1 + u'_0 - \left[\xi \left(1 - \frac{\psi^2}{2} \right) + \eta \psi \right] \phi' + (\xi \psi \psi' - \eta \psi') \phi \right\} dx - \psi \phi d\eta - \left(1 - \frac{\psi^2}{2} \right) \phi d\xi \quad (6a)$$

$$dy_1 = -(\eta \psi \psi' + \xi \psi') dx + \left(1 - \frac{\psi^2}{2} \right) d\eta - \psi d\xi \quad (6b)$$

$$dz_1 = (w' - \xi \psi \psi' + \eta \psi') dx + \psi d\eta + \left(1 - \frac{\psi^2}{2} \right) d\xi \quad (6c)$$

Here, dx , $d\eta$ and $d\xi$ are the increments along the deformed elastic axis and two cross sectional axes, respectively.

The classical strain tensor ε_{ij} may be obtained using the equilibrium equation below Eringen (1980)

$$d\vec{r}_1 \cdot d\vec{r}_1 - d\vec{r}_0 \cdot d\vec{r}_0 = 2 \left[\begin{matrix} dx & d\eta & d\xi \end{matrix} \right] \left[\varepsilon_{ij} \right] \left\{ \begin{matrix} dx \\ d\eta \\ d\xi \end{matrix} \right\} \quad (7)$$

$$\text{where } \left[\varepsilon_{ij} \right] = \begin{bmatrix} \varepsilon_{xx} & \varepsilon_{x\eta} & \varepsilon_{x\xi} \\ \varepsilon_{\eta x} & \varepsilon_{\eta\eta} & \varepsilon_{\eta\xi} \\ \varepsilon_{\xi x} & \varepsilon_{\xi\eta} & \varepsilon_{\xi\xi} \end{bmatrix}.$$

Substituting equations (5a)-(6c) into equation (7), the components of the strain tensor ε_{ij} are obtained as follows

$$2\gamma_{xx} = \left\{ 1 + u'_0 - \left[\xi \left(1 - \frac{\psi^2}{2} \right) + \eta\psi \right] \varphi' + (\xi\psi\psi' - \eta\psi')\varphi \right\}^2 + (\eta\psi\psi' + \xi\psi')^2 + (w' - \xi\psi\psi' + \psi'\eta)^2 - 1 \quad (8a)$$

$$2\gamma_{x\eta} = - \left\{ 1 + u'_0 - \left[\xi \left(1 - \frac{\psi^2}{2} \right) + \eta\psi \right] \varphi' + (\xi\psi\psi' - \eta\psi')\varphi \right\} (\psi\varphi) - (\eta\psi\psi' + \xi\psi') \left(1 - \frac{\psi^2}{2} \right) + (w' - \xi\psi\psi' + \eta\psi')\psi \quad (8b)$$

$$2\gamma_{x\xi} = - \left\{ 1 + u'_0 - \left[\xi \left(1 - \frac{\psi^2}{2} \right) + \eta\psi \right] \varphi' + (\xi\psi\psi' - \eta\psi')\varphi \right\} \left(1 - \frac{\psi^2}{2} \right) \varphi + (\eta\psi\psi' + \xi\psi')\psi + (w' - \xi\psi\psi' + \eta\psi') \left(1 - \frac{\psi^2}{2} \right) \quad (8c)$$

In this study, γ_{xx} , $\gamma_{x\eta}$ and $\gamma_{x\xi}$ are used in the calculations because as noted by Hodges and Dowell (1974) for long slender beams, the axial strain ε_{xx} is dominant over the transverse normal strains, $\varepsilon_{\eta\eta}$ and $\varepsilon_{\xi\xi}$. Additionally, the shear strain $\varepsilon_{\eta\xi}$ is two order smaller than the other shear strains, $\varepsilon_{x\eta}$ and $\varepsilon_{x\xi}$.

In order to obtain simpler expressions for the strain components, higher order terms should be neglected so an order of magnitude analysis is performed by using the ordering scheme, taken from Hodges and Dowell (1974) and introduced in Table 1. Hodges and Dowell (1974) used the formulation for an Euler-Bernoulli beam. In this study, their formulation is modified for a Timoshenko beam and the following expression is added to their ordering scheme as a contribution to literature,

$$\gamma = w' - \varphi = O(\varepsilon^2) \quad (9)$$

Considering Table 1, the following simplified strain expressions are obtained.

$$\varepsilon_{xx} = u'_0 - \xi\varphi' + \frac{1}{2}(w')^2 + \frac{1}{2}(\eta^2 + \xi^2)(\psi')^2 \quad (10a)$$

$$\gamma_{x\eta} = -\xi\psi' \quad (10b)$$

$$\gamma_{x\xi} = w' - \varphi + \eta\psi' \quad (10c)$$

TABLE 1

The expression for the potential energy due to bending and torsion, U_{bt} , is given by

$$U_{bt} = \frac{1}{2} \int_0^L \left(\iint_A E \varepsilon_{xx}^2 d\eta d\xi \right) dx \quad (11)$$

where A is the cross-section area and E is the Young's modulus.

Substituting equation (10a) into equation (11), the following expression is obtained.

$$U_{bt} = \frac{1}{2} \int_0^L \left(\iint_A E \left\{ u'_0 - \xi\varphi' + \frac{1}{2}(w')^2 + \frac{1}{2}(\eta^2 + \xi^2)(\psi')^2 \right\}^2 d\eta d\xi \right) dx \quad (12)$$

Taking integration over the blade cross-section and referring to the definitions given in Table 2, the following bending-torsion potential energy expression is obtained.

$$U_{bt} = \frac{1}{2} \int_0^L EA(u'_0)^2 dx + \frac{1}{2} \int_0^L EI_y(\varphi')^2 dx + \frac{1}{2} \int_0^L EAu'_0(w')^2 dx + \frac{1}{2} \int_0^L I_\alpha \frac{u'_0}{\rho} (\psi')^2 dx \quad (13)$$

where the mass moment of inertia about the elastic axis, I_α , is given by

$$I_\alpha = \iint_A \rho(\eta^2 + \xi^2) d\eta d\xi \quad (14)$$

TABLE 2

The uniform strain ε_0 and the associated axial displacement u_0 due to the centrifugal force $T(x)$ is given by

$$u'_0(x) = \varepsilon_0(x) = \frac{T(x)}{EA} \quad (15)$$

where the centrifugal force is expressed as follows

$$T(x) = \int_x^L \rho A \Omega^2 (R + x) dx \quad (16)$$

Substituting equations (15) and (16) into equation (13) and noting that the

$\frac{1}{2} \int_0^L \frac{T^2(x)}{EA} dx$ term is constant and will be denoted with β , the final form of the bending-

torsion potential energy is obtained as follows

$$U_{bt} = \frac{1}{2} \int_0^L EI_y (\varphi')^2 dx + \frac{1}{2} \int_0^L T \left[(w')^2 + \frac{I_\alpha}{\rho A} (\psi')^2 \right] dx + \beta \quad (17)$$

The expression for the potential energy due to shear, U_s , is given by

$$U_s = \frac{1}{2} \int_0^L \left(\iint_A G (\gamma_{x\eta}^2 + \gamma_{x\xi}^2) d\eta d\xi \right) dx \quad (18)$$

where G is the shear modulus.

Substituting equations (10b) and (10c) into equation (18), the following expression for the potential energy due to shear is obtained.

$$U_s = \frac{1}{2} \int_0^L \left(\iint_A G [\xi^2 (\psi')^2 + (w' - \varphi + \eta \psi')^2] d\eta d\xi \right) dx \quad (19)$$

Using the definitions given by Table 2, equation (19) can be rewritten as follows

$$U_s = \frac{1}{2} \int_0^L \{ kAG (w' - \varphi)^2 dx + GJ (\psi')^2 \} dx \quad (20)$$

where k is the shear correction factor, kAG is the shear rigidity and GJ is the torsional rigidity of the beam cross section.

Summing equations (17) and (20), the total potential energy expression is given by

$$U = \frac{1}{2} \int_0^L \left\{ EI_y (\varphi')^2 + T \left[(w')^2 + \frac{I_\alpha}{\rho A} (\psi')^2 \right] + kAG (w' - \varphi)^2 + GJ (\psi')^2 + \beta \right\} dx \quad (21)$$

3.2. Derivation of the Kinetic Energy Expression

The velocity vector of the point P is given by

$$\vec{V} = \frac{\partial \vec{r}}{\partial t} + \Omega \vec{k} \times \vec{r} \quad (22)$$

where

$$\vec{r} = x_1 \vec{i} + y_1 \vec{j} + z_1 \vec{k} \quad (23)$$

Substituting equation (23) into equation (22), the total velocity vector expression is obtained as follows

$$\vec{V} = (\dot{x}_1 - \Omega y_1) \vec{i} + (\dot{y}_1 + \Omega x_1) \vec{j} + \dot{z}_1 \vec{k} \quad (24)$$

where \dot{x}_1 , \dot{y}_1 and \dot{z}_1 are the derivatives of the coordinates with respect to time, t .

Substituting equations (3a)-(3c) into equation (24) and applying the ordering scheme given by Table 1, the velocity components are obtained as follows

$$V_x = -\left[\xi \left(1 - \frac{\psi^2}{2}\right) + \eta \psi \right] \dot{\phi} + (\xi \psi \dot{\psi} - \eta \dot{\psi}) \phi - \left[\eta \left(1 - \frac{\psi^2}{2}\right) - \xi \psi \right] \Omega \quad (25a)$$

$$V_y = -(\eta \psi + \xi) \dot{\psi} + \left\{ R + x + u_0 - \left[\xi \left(1 - \frac{\psi^2}{2}\right) + \eta \psi \right] \phi \right\} \Omega \quad (25b)$$

$$V_z = \dot{w} + (\eta - \xi \psi) \dot{\psi} \quad (25c)$$

The general expression of the kinetic energy is

$$\mathfrak{T} = \frac{1}{2} \int_0^L \left(\iint_A \rho (V_x^2 + V_y^2 + V_z^2) d\eta d\xi \right) dx \quad (26)$$

Substituting equations (25a)-(25c) into equation (26) and using the definitions given in Table 3, the following kinetic energy expression is obtained.

$$\begin{aligned} \mathfrak{S} = \frac{1}{2} \int_0^L \{ & \rho A \dot{w}^2 + \rho I_y [\Omega^2 \varphi^2 + \dot{\varphi}^2 + 2\Omega(\varphi\dot{\psi} - \dot{\varphi}\psi)] + I_\alpha \dot{\psi}^2 + \rho(I_y - I_z)\Omega^2 \psi^2 + \\ & 2\rho I_z \Omega(\varphi\dot{\psi} + \dot{\varphi}\psi) + 2\rho A e [\dot{w}\dot{\psi} - (R+x)\Omega^2 \psi \varphi] \} dx \end{aligned} \quad (27)$$

In most cases Coriolis terms can be ignored so equation (27) reduces to its final form as follows.

$$\begin{aligned} \mathfrak{S} = \frac{1}{2} \int_0^L \{ & \rho A \dot{w}^2 + \rho I_y (\Omega^2 \varphi^2 + \dot{\varphi}^2) + I_\alpha \dot{\psi}^2 + \rho(I_y - I_z)\Omega^2 \psi^2 + \\ & 2\rho A e [\dot{w}\dot{\psi} - (R+x)\Omega^2 \psi \varphi] \} dx \end{aligned} \quad (28)$$

TABLE 3

3.3. Governing Differential Equations of Motion

The governing differential equations of motion and the associated boundary conditions are obtained applying the Hamilton's principle, given below, to the derived energy expressions.

$$\int_{t_1}^{t_2} \delta(U - \mathfrak{S} - W) dt = 0 \quad (29)$$

In this study, undamped, free vibration analysis is performed so variation of the the virtual work that is done by the nonconservative forces, δW , is zero in equation (29). Therefore, variation of the kinetic and potential energy expressions are taken and substituted into equation (29).

Using variational principles, the equations of motions for a rotating, uniform Timoshenko beam with bending-torsion coupling are derived as follows

$$\rho A \ddot{w} + \rho A e \ddot{\psi} - (T w')' - [k A G (w' - \varphi)]' = 0 \quad (30a)$$

$$\rho I_y \ddot{\varphi} - \rho I_y \Omega^2 \varphi - (E I_y \varphi')' - k A G (w' - \varphi) - 2\rho I_y \Omega \dot{\psi} + \rho A e \Omega^2 (R+x)\psi = 0 \quad (30b)$$

$$I_\alpha \ddot{\psi} + \rho A e \ddot{w} - \rho(I_y - I_z)\Omega^2 \psi - (GJ\psi')' - \left(\frac{TI_\alpha}{\rho A}\psi'\right)' + 2\rho I_y \Omega \dot{\varphi} + \rho A e \Omega^2 (R+x)\varphi = 0 \quad (30c)$$

Here, w is the flapwise bending displacement, φ is the rotation due to bending and ψ is the torsion angle.

In the preparation stage of this study, formulation was carried out by both including and excluding the Coriolis terms that are $2\rho I_y \Omega \dot{\psi}$ and $2\rho I_y \Omega \dot{\varphi}$. Considering the time spent by Mathematica to calculate the natural frequencies, it is noticed that although the results of both formulation are very similar, calculations made by including the Coriolis terms takes much longer time than the ones made by excluding this term. Therefore, the equations of motion that do not include the Coriolis terms are used in the formulation.

Neglecting the Coriolis terms, equations (30a)-(30c) reduce to

$$\rho A \ddot{w} + \rho A e \ddot{\psi} - (Tw')' - [kAG(w' - \varphi)]' = 0 \quad (31a)$$

$$\rho I_y \ddot{\varphi} - \rho I_y \Omega^2 \varphi - (EI_y \varphi')' - kAG(w' - \varphi) + \rho A e \Omega^2 (R+x)\psi = 0 \quad (31b)$$

$$I_\alpha \ddot{\psi} + \rho A e \ddot{w} - \rho(I_y - I_z)\Omega^2 \psi - (GJ\psi')' - \left(\frac{TI_\alpha}{\rho A}\psi'\right)' + \rho A e \Omega^2 (R+x)\varphi = 0 \quad (31c)$$

Additionally, after the application of the Hamilton's principle, the boundary conditions are obtained as follows

- The geometric boundary conditions at the cantilever end, $x = 0$, of the Timoshenko beam,

$$w(0, t) = \varphi(0, t) = \psi(0, t) = 0 \quad (32a)$$

- The natural boundary conditions at the free end, $x = L$, of the Timoshenko beam,

$$\text{Shear force:} \quad Tw' + kAG(w' - \varphi) = 0 \quad (32b)$$

$$\text{Bending Moment: } EI_y \varphi' = 0 \quad (32c)$$

$$\text{Torsion: } GJ\psi' = 0 \quad (32d)$$

The boundary conditions expressed by Eqs. (32b)-(32d) can be written in a simpler form by noting that the centrifugal force is zero at the free end of the beam, $T(L) = 0$.

$$w' - \varphi = 0 \quad (33a)$$

$$\varphi' = 0 \quad (33b)$$

$$\psi' = 0 \quad (33c)$$

In this paper, a uniform beam is investigated so the cross-sectional area and moments of inertia do not change with respect to the spanwise direction, x as is the case in a tapered beam problem so the governing differential equations of motion can be rewritten as follows

$$\rho A \ddot{w} + \rho A e \ddot{\psi} - (T w')' - k A G (w'' - \varphi') = 0 \quad (34a)$$

$$\rho I_y \ddot{\varphi} - \rho I_y \Omega^2 \varphi - EI_y \varphi'' - k A G (w' - \varphi) + \rho A e \Omega^2 (R + x) \psi = 0 \quad (34b)$$

$$I_\alpha \ddot{\psi} + \rho A e \ddot{w} - \rho (I_y - I_z) \Omega^2 \psi - G J \psi'' - \frac{I_\alpha}{\rho A} (T \psi')' + \rho A e \Omega^2 (R + x) \varphi = 0 \quad (34c)$$

4. Vibration Analysis

4.1. Harmonic Motion Assumption and Dimensionless Parameters

In order to investigate the undamped free vibration of the beam model considered in this study, a sinusoidal variation of $w(x, t)$, $\psi(x, t)$ and $\varphi(x, t)$ with a circular natural frequency, ω , is assumed and the functions are taken as

$$w(x, t) = \overline{W}(x) e^{i\omega t} \quad (35a)$$

$$\psi(x, t) = \bar{\psi}(x)e^{i\omega t} \quad (35b)$$

$$\varphi(x, t) = \bar{\varphi}(x)e^{i\omega t} \quad (35c)$$

Substituting equations (35a)-(35c) into equations (34a)-(34c) results in the following expressions

$$\rho A \omega^2 \bar{W} + \rho A e \omega^2 \bar{\psi} + (T\bar{W}')' + kAG(\bar{W}'' - \bar{\varphi}') = 0 \quad (36a)$$

$$\rho I_y \omega^2 \bar{\varphi} + \rho I_y \Omega^2 \bar{\varphi} + EI_y \bar{\varphi}'' + kAG(W' - \bar{\varphi}) - \rho A e \Omega^2 (R + x) \bar{\psi} = 0 \quad (36b)$$

$$I_\alpha \omega^2 \bar{\psi} + \rho A e \omega^2 \bar{W} + \rho(I_y - I_z) \Omega^2 \bar{\psi} + GJ \bar{\psi}'' + \frac{I_\alpha}{\rho A} (T\bar{\psi}')' - \rho A e \Omega^2 (R + x) \bar{\varphi} = 0 \quad (36c)$$

In order to make comparisons with open literature, the following dimensionless parameters are introduced.

$$\begin{aligned} \bar{x} &= \frac{x}{L} & \delta &= \frac{R}{L} & \bar{e} &= \frac{e}{L} & \bar{\Omega}^2 &= \frac{\rho A L^4 \Omega^2}{EI_y} & \mu^2 &= \frac{\rho A L^4 \omega^2}{EI_y} \\ r^2 &= \frac{1}{S^2} = \frac{I_y}{AL^2} & r_\alpha^2 &= \frac{I_\alpha}{\rho A L^2} & s^2 &= \frac{EI_y}{kAGL^2} & \varepsilon^2 &= \frac{GJ}{EI_y} & \tilde{W} &= \frac{\bar{W}}{L} \end{aligned} \quad (37)$$

Substituting these dimensionless parameters into equations (36a)-(36c), the dimensionless equations of motion are expressed as follows

$$\frac{d}{d\bar{x}} \left\{ \left[\delta(1-\bar{x}) + \frac{1}{2}(1-\bar{x}^2) \right] \frac{d\tilde{W}}{d\bar{x}} \right\} + A_1 \frac{d^2 \tilde{W}}{d\bar{x}^2} + A_2 \tilde{W} + A_3 \frac{d\bar{\varphi}}{d\bar{x}} + A_4 \bar{\psi} = 0 \quad (38a)$$

$$\frac{d^2 \bar{\varphi}}{d\bar{x}^2} + B_1 \bar{\varphi} + B_2 \frac{d\tilde{W}}{d\bar{x}} + B_3 \bar{\psi} + B_4 \bar{x} \bar{\psi} = 0 \quad (38b)$$

$$\frac{d}{d\bar{x}} \left\{ \left[\delta(1-\bar{x}) + \frac{1}{2}(1-\bar{x}^2) \right] \frac{d}{d\bar{x}} \bar{\psi} \right\} + C_1 \frac{d^2 \bar{\psi}}{d\bar{x}^2} + C_2 \bar{\psi} + C_3 \bar{\varphi} + C_4 \bar{x} \bar{\varphi} + C_5 \tilde{W} = 0 \quad (38c)$$

where the coefficients are given by

$$A_1 = \frac{1}{s^2 \bar{\Omega}^2}, \quad A_2 = \frac{\mu^2}{\bar{\Omega}^2}, \quad A_3 = -\frac{1}{s^2 \bar{\Omega}^2}, \quad A_4 = \bar{e} \frac{\mu^2}{\bar{\Omega}^2} \quad (39a)$$

$$B_1 = \bar{\Omega}^2 r^2 \left(1 + \frac{\mu^2}{\bar{\Omega}^2}\right) - \frac{1}{s^2}, \quad B_2 = \frac{1}{s^2}, \quad B_3 = -\bar{e} \bar{\Omega}^2 \delta, \quad B_4 = -\bar{e} \bar{\Omega}^2 \quad (39b)$$

$$C_1 = \frac{\varepsilon^2}{\bar{\Omega}^2 r_a^2}, \quad C_2 = \frac{\mu^2}{\bar{\Omega}^2} + 2 \frac{r^2}{r_a^2} - 1, \quad C_3 = -\frac{\delta}{r_a^2} \bar{e}, \quad C_4 = -\frac{1}{r_a^2} \bar{e}, \quad C_5 = \frac{1}{r_a^2} \frac{\mu^2}{\bar{\Omega}^2} \bar{e} \quad (39c)$$

4.2. The Differential Transform Method

The Differential Transform Method, DTM, is a transformation technique based on the Taylor series expansion and is a useful tool to obtain analytical solutions of the differential equations. In this method, certain transformation rules are applied and the governing differential equations and the boundary conditions of the system are transformed into a set of algebraic equations in terms of the differential transforms of the original functions and the solution of these algebraic equations gives the desired solution of the problem. It is different from high-order Taylor series method because Taylor series method requires symbolic computation of the necessary derivatives of the data functions and is expensive for large orders. Details of the application procedure of DTM is explained by Ozdemir Ozgumus and Kaya (2006b) using several explanatory tables.

4.3. Formulation with DTM

In the solution step, the differential transform method is applied to equations (38a)-(38c) at $x_0 = 0$ and the following transformed expressions are obtained.

$$A_1(k+2)(k+1)\varphi[k+2] + A_2\varphi[k] + A_3(k+1)\mathcal{W}[k+1] + A_4(k+2)(k+1)\psi[k+2] = 0 \quad (40a)$$

$$B_1(k+2)(k+1)\mathcal{W}[k+2] + B_2\mathcal{W}[k] + B_3(k+1)\varphi[k+1] = 0 \quad (40b)$$

$$C_1(k+2)(k+1)\psi[k+2] + C_2\psi[k] + C_3(k+2)(k+1)\varphi[k+2] = 0 \quad (40c)$$

Applying DTM to equations (32a)–(33c), the transformed boundary conditions are obtained as follows

$$\text{at } \bar{x} = 0 \quad \Rightarrow \quad \varphi[0] = W[0] = \psi[0] = 0 \quad (41a)$$

$$\text{at } \bar{x} = 1 \quad \Rightarrow \quad (k+1)\varphi[k+1] + A_4(k+1)\psi[k+1] = 0 \quad (41b)$$

$$B_1(k+1)W[k+1] - \varphi[k] = 0 \quad (41c)$$

$$C_1(k+1)\psi[k+1] + C_3(k+1)\varphi[k+1] = 0 \quad (41d)$$

Substituting the boundary conditions expressed in equations (41a)-(41d) into equations (40a)-(40c) and taking $\varphi[1] = d_1$, $W[1] = d_2$, $\psi[1] = d_3$, the following expression is obtained

$$A_{j1}^{(n)}(\omega)d_1 + A_{j2}^{(n)}(\omega)d_2 + A_{j3}^{(n)}(\omega)d_3 = 0, \quad j = 1, 2, 3 \quad (42)$$

where d_1, d_2 and d_3 are constants and $A_{j1}^{(n)}(\omega), A_{j2}^{(n)}(\omega), A_{j3}^{(n)}(\omega)$ are polynomials of ω corresponding to n .

The matrix form of equation (42) can be given by

$$\begin{bmatrix} A_{11}^{(n)}(\omega) & A_{12}^{(n)}(\omega) & A_{13}^{(n)}(\omega) \\ A_{21}^{(n)}(\omega) & A_{22}^{(n)}(\omega) & A_{23}^{(n)}(\omega) \\ A_{31}^{(n)}(\omega) & A_{32}^{(n)}(\omega) & A_{33}^{(n)}(\omega) \end{bmatrix} \begin{Bmatrix} d_1 \\ d_2 \\ d_3 \end{Bmatrix} = \begin{Bmatrix} 0 \\ 0 \\ 0 \end{Bmatrix} \quad (43)$$

The eigenvalues are calculated by taking the determinant of the $[A_{ji}]$ matrix.

$$\begin{vmatrix} A_{11}^{(n)}(\omega) & A_{12}^{(n)}(\omega) & A_{13}^{(n)}(\omega) \\ A_{21}^{(n)}(\omega) & A_{22}^{(n)}(\omega) & A_{23}^{(n)}(\omega) \\ A_{31}^{(n)}(\omega) & A_{32}^{(n)}(\omega) & A_{33}^{(n)}(\omega) \end{vmatrix} = 0 \quad (44)$$

Solving equation (44), the eigenvalues are calculated. The j^{th} estimated eigenvalue, $\omega_j^{(n)}$ corresponds to n and the value of n is determined by the following equation:

$$\left| \omega_j^{(n)} - \omega_j^{(n-1)} \right| \leq \varepsilon \quad (45)$$

where $\omega_j^{(n-1)}$ is the j^{th} estimated eigenvalue corresponding to $n-1$ and where ε is the tolerance parameter.

If equations (45) is satisfied, then the j^{th} eigenvalue, $\omega_j^{(n)}$, is obtained. In general, $\omega_j^{(n)}$ are conjugated complex values, and can be written as $\omega_j^{(n)} = a_j + ib_j$. Neglecting the small imaginary part b_j , the j^{th} natural frequency, a_j , is found.

5. Results and Discussions

At first glance, application of DTM to both the equations of motion and the boundary conditions seems to be very involved computationally. However, all the algebraic calculations are finished quickly by using a symbolic computational software. Therefore, the computer package Mathematica is used to write a code for the expressions given by equations (40a)-(41d). The natural frequencies are calculated, the mode shapes are plotted and the effects of the rotational speed, rotary inertia, shear deformation, slenderness ratio and bending-torsion coupling are investigated. Additionally, in order to validate the calculated results, a rotating uniform Timoshenko beam that features bending-torsion coupling is created and analysed in the finite element program, ABAQUS and two illustrative examples which study simpler beam models are found in open literature and solved in order to make comparisons. Consequently, it is observed that there is a good agreement between the results.

In Figures 4 (a-f), the first six normal mode shapes of a rotating uniform Timoshenko beam featuring bending-torsion coupling are introduced. As it is seen here, the first four

and the sixth modes are dominated by bending (w and φ) while in the fifth mode, torsion (ψ) is dominant.

FIGURES 4 (a-f)

In Figure 5, convergence of the first five natural frequencies with respect to the number of terms, N , used in DTM application is introduced. To evaluate up to the fifth natural frequency to five-digit precision, it was necessary to take 30 terms. During the calculations, it is noticed that when the rotational speed parameter is increased, the number of the terms has to be increased to achieve the same accuracy. Additionally, here it is seen that higher modes appear when more terms are taken into account in DTM application. Thus, depending on the order of the required mode, one must try a few values for the term number at the beginning of the Mathematica calculations in order to find the adequate number of terms.

FIGURE 5

In Table 4, variation of the first six natural frequencies, ω , with respect to the rotational speed, Ω , is tabulated in Table 4 for the beam properties given below. Additionally, the results taken from ABAQUS are included and it is observed that there is a good agreement between the results of this study and the ABAQUS results.

$$\begin{array}{llll}
 GJ = 95118 \text{ Nm}^2 & I_\alpha = 0.131 \text{ kgm} & EI = 65563.7 \text{ Nm}^2 & \\
 kAG = 2.015 \times 10^8 \text{ N} & \rho A = 27.2527 \text{ kg/m} & e = 0.0155 \text{ m} & L = 5 \text{ m}
 \end{array}$$

TABLE 4

Here it is seen that the natural frequencies increase with the increasing rotational speed because of the stiffening effect of the centrifugal force, equation (16), that is proportional to the square of the angular speed. The increase in the frequency due to rotation is 69 %

for the first bending mode, 35 % for the second bending mode, 17 % for the third bending mode, 11 % for the fourth bending mode and 7 % for the fifth bending mode. Comparing the percentage increase in the bending frequencies, it is noticed that the effect of the rotational speed is dominant on the fundamental bending mode and this effect diminishes rapidly as the frequency order increases. Moreover, the increase of frequency due to rotation is 0.34 % for the torsion dominated mode. Therefore, the effect of rotation on the torsion dominated modes is insignificant even when it is compared with the low bending dominated frequencies.

For further validation, in Table 5, the results are compared with the ones calculated by Sabuncu and Evran (2005) and Eslimy-Isfahany and Banerjee (2000) for the values given below.

For Sabuncu and Evran (2005),

$$\begin{array}{llll}
 GJ = 9.14 \text{ Nm}^2 & I_z = 34.96 \times 10^{-12} \text{ m}^4 & I_y = 2.7928 \times 10^{-9} \text{ m}^4 & k = 0.833 \\
 E = 213.9 \times 10^9 \text{ N/m}^2 & R = 0.0762 \text{ m} & L = 0.1524 \text{ m} & e = 0 \text{ m} \\
 \rho = 7859 \text{ kg/m}^3 & A = 58.97 \times 10^{-6} \text{ m}^2 & &
 \end{array}$$

where a nonrotating uniform Timoshenko beam that is uncoupled is considered.

For Eslimy-Isfahany and Banerjee (2000),

$$\begin{array}{lll}
 GJ = 9.88 \times 10^5 \text{ Nm}^2 & EI_y = 9.75 \times 10^6 \text{ Nm}^2 & I_\alpha = 8.65 \text{ kgm} \\
 \rho A = 35.75 \text{ kg/m} & kAG = 296154000 \text{ N} & e = -0.18 \text{ m} \\
 L = 6 \text{ m} & &
 \end{array}$$

where a nonrotating, uniform Timoshenko beam featuring bending-torsion coupling is considered.

TABLE 5

In Table 6, effects of the bending-torsion coupling, rotary inertia and shear deformation are tabulated. Examining Table 6, the following results are obtained:

- As noted by Subrahmanyam et. al. (1981), bending-torsion coupling has a decreasing effect on the bending dominated natural frequencies (the first four and the sixth modes) while it has an increasing effect on the torsion dominated frequencies (the fifth mode).

- Rotary inertia and shear deformation effects that are results of the Timoshenko Beam Theory have a decreasing effect on the bending dominated natural frequencies. Therefore, the bending dominated natural frequencies of the coupled Timoshenko beam are lower than the natural frequencies of the coupled Euler-Bernoulli beam. However, rotary inertia and shear deformation have almost no effect on the torsion dominated natural frequencies.

- Both the coupling effect and the Timoshenko effects are more significant on the higher modes.

TABLE 6

In Table 7, effect of the Coriolis terms, $2\rho I_y \Omega \dot{\psi}$ and $2\rho I_y \Omega \dot{\phi}$, on the natural frequencies are introduced. Here it is observed that these terms are not very effective even when the hub rotates at very high Ω values. Considering the time spent by Mathematica to calculate the natural frequencies, it is noticed that although the results are very similar, calculations made by including the Coriolis terms takes much longer time

than the ones made by excluding this term. Therefore, these terms have not been included in the calculations of this study.

REFERENCES

- Banerjee, J.R., Williams, F.W., 1994, "Coupled bending-torsional dynamic stiffness matrix of an axially loaded Timoshenko beam element, *International Journal of Solids and Structures*, 31 (6), 749-762.
- Banerjee, J.R., Williams, F.W., 1992, "Coupled bending-torsional dynamic stiffness matrix for Timoshenko beam elements", *Computers & Structures*, 42 (3), 301-310
- Banerjee, J.R., Guo S., Howson W.P., 1996, Exact dynamic stiffness matrix of a bending-torsion coupled beam including warping, *Computers & Structures*, 59 (4), 613-621.
- Bercin A. N. and Tanaka M., 1997, "Coupled flexural-torsional vibrations of Timoshenko beams", *Journal of Sound and Vibration*, 207 (1) 47-59.
- Bishop R. E. D., Cannon S. M. and Miao S., 1989, "On coupled bending and torsional vibration of uniform beams", *Journal of Sound and Vibration*, 131, 457-464.
- Bishop R.E.D., Price W.G., 1977, "Coupled bending and twisting of a Timoshenko beam, *Journal of Sound and Vibration*, 50 (4), 469-477.
- Dokumacı E., 1987, "An exact solution for coupled bending and torsion vibrations of uniform beams having single cross-sectional symmetry", *Journal of Sound and Vibration*, 119, 443-449.
- Eslimy-Isfahany S. H. R. and Banerjee J. R., 2000, "Use of generalized mass in the interpretation of dynamic response of bending torsion coupled beams", *Journal of Sound and Vibration*, 238(2), 295-308.
- Eslimy-Isfahany S.H.R., Banerjee, J.R., Sobey A.J., 1996, Response of a bending-torsion coupled beam to deterministic and random loads, *Journal of Sound and Vibration*, 195 (2), 267-283.
- Hallauer, W.L., Liu, R.Y.L., 1982, Beam bending-torsion dynamic stiffness method for calculation of exact vibration modes, *Journal of Sound and Vibration*, 85 (1), 105-113.
- Hashemi, S.M., Richard, M.J., 2000, "Free vibrational analysis of axially loaded bending-torsion coupled beams: a dynamic finite element", *Computers & Structures*, 77(6), 711-724.
- Hodges D.H. and Ormiston A. R., 1976, "Stability of elastic bending and torsion of uniform cantilever rotor blades in hover with variable structural coupling, NASA TN D - 8192.
- Hodges D.H. and Dowell E. H., 1974, "Nonlinear equations of motion for the elastic bending and torsion of twisted nonuniform rotor blades", NASA TN D -7818.

Houbolt J.C. and Brooks G.W., 1957, "Differential equations of motion for combined flapwise bending, chordwise bending and torsion of twisted nonuniform rotor blades", Report 1346, NACA Technical Note.

Kaya M.O., 2006, "Free vibration analysis of rotating Timoshenko beams by differential transform method", *Aircraft Engineering and Aerospace Technology: An International Journal*, 78 (3), 194-203.

Özdemir Ö. and Kaya M.O., 2006a, "Flexural vibration analysis of double tapered rotating Euler-Bernoulli beam by using the differential transform method", *MECCANICA*, 41(6), 661-670.

Özdemir Ö. and Kaya M.O., 2006b, "Flapwise bending vibration analysis of a rotating tapered cantilevered Bernoulli-Euler beam by differential transform method", *Journal of Sound and Vibration*, 289, 413-420.

Prokić A., 2006, "On fivefold coupled vibrations of Timoshenko thin-walled beams", *Engineering Structures*, 28 (1), 54-62.

Sabuncu M. and Evran K., 2005, "Dynamic stability of a rotating asymmetric cross-section Timoshenko beam subjected to an axial periodic force", *Finite Elements in Analysis and Design*, 41 (11-12), 1011-1026

Subrahmanyam K. B., Kulkarni S. V. and Rao J. S., 1981, "Coupled bending-bending vibrations of pre-twisted cantilever blading allowing for shear deflection and rotary inertia by the Reissner method", *International Journal of Mechanical Sciences*, 23 (9), 517-530

Yaman Y., 1997, "Vibrations of open-section channels: A coupled flexural and torsional wave analysis", *Journal of Sound and Vibration*, 204, 131-158.

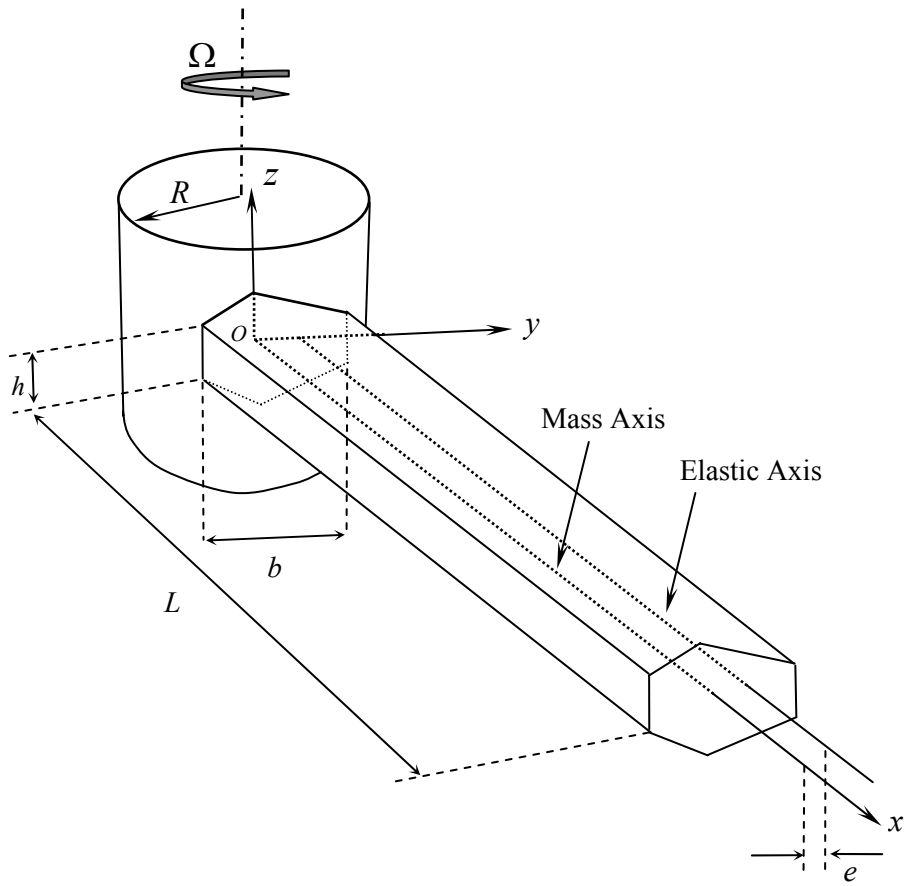


Figure 1. Configuration of A Uniform, Rotating, Cantilever Timoshenko Beam Featuring Bending-Torsion Coupling

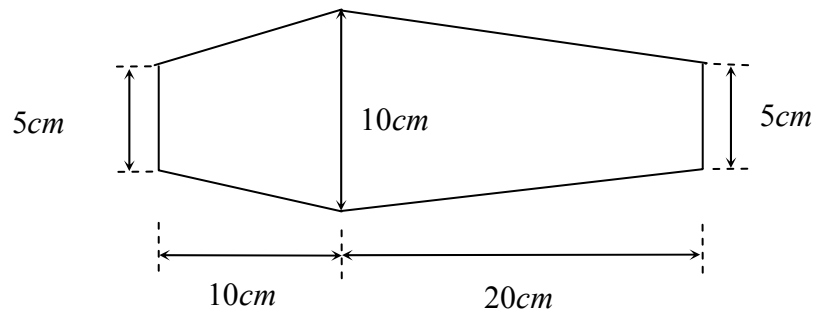


Figure 2. The Cross-Sectional View and Dimensions the Uniform Timoshenko Beam with One Symmetry Axis

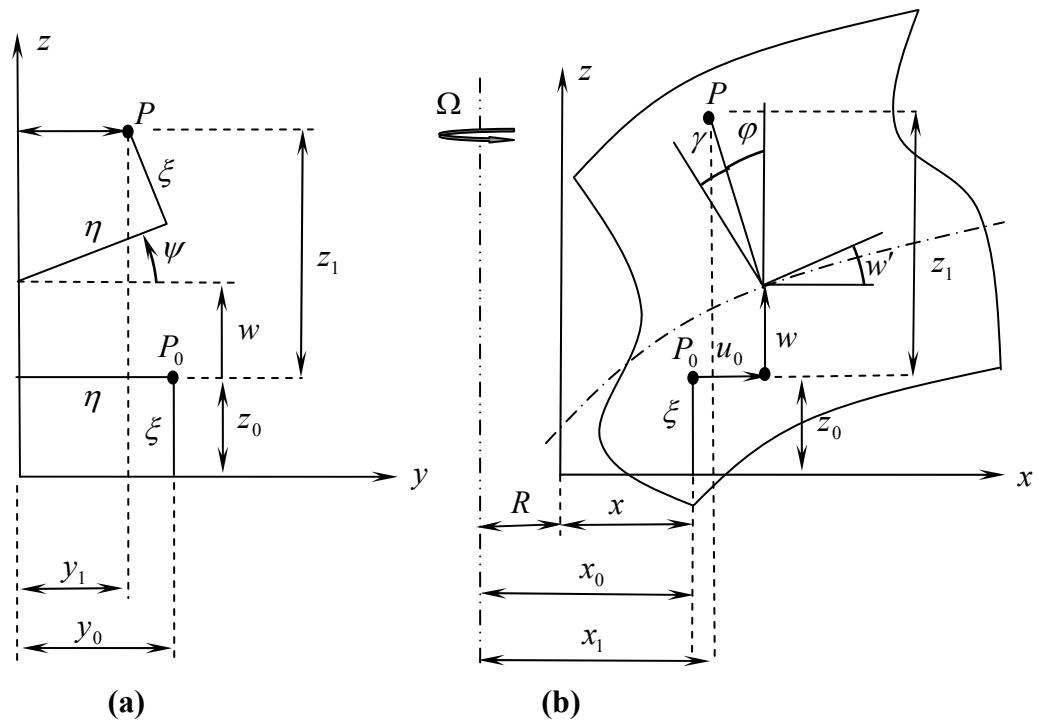
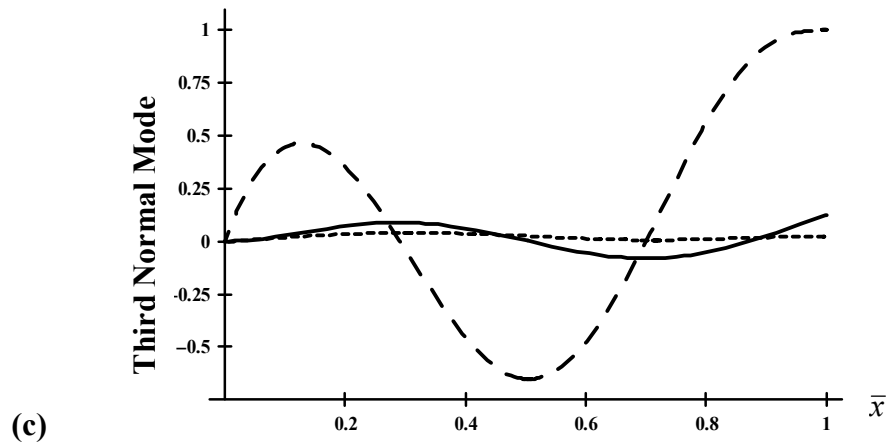
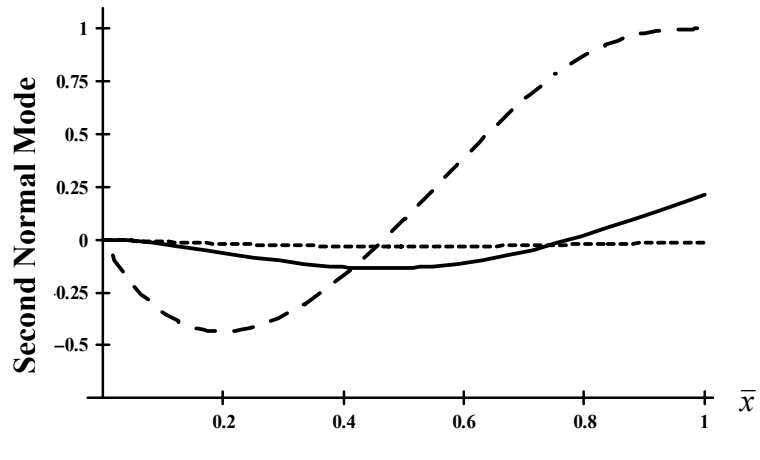
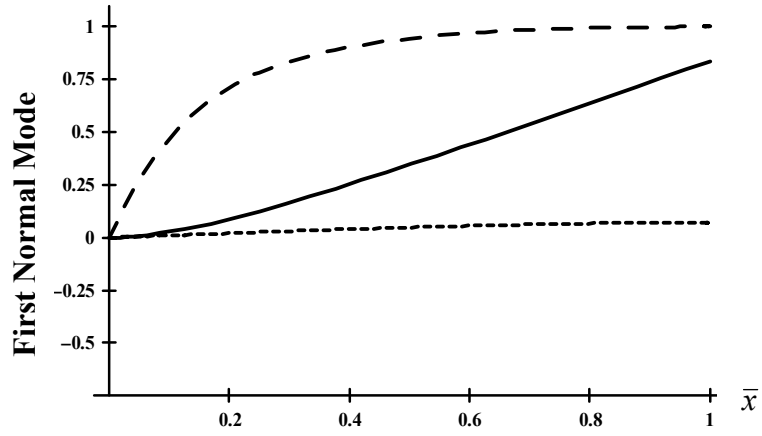


Figure 3. (a) Cross-Sectional View (b) Side View of the Bending-Torsion Deflections of The Reference Point



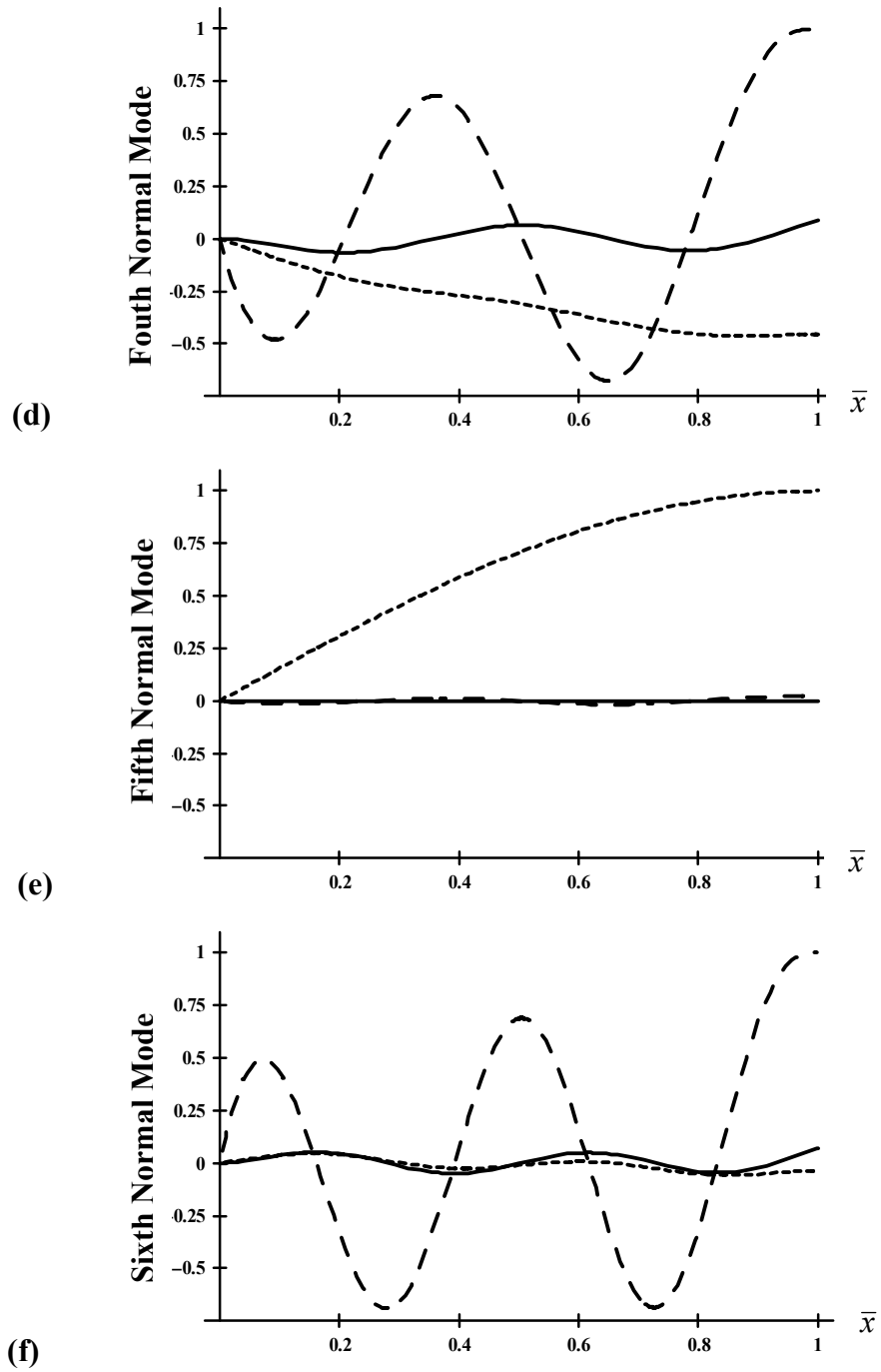


Figure 4. The Normal Mode Shapes of The Rotating Coupled Timoshenko Beam

(——— , w ; - - - , φ ; , ψ)

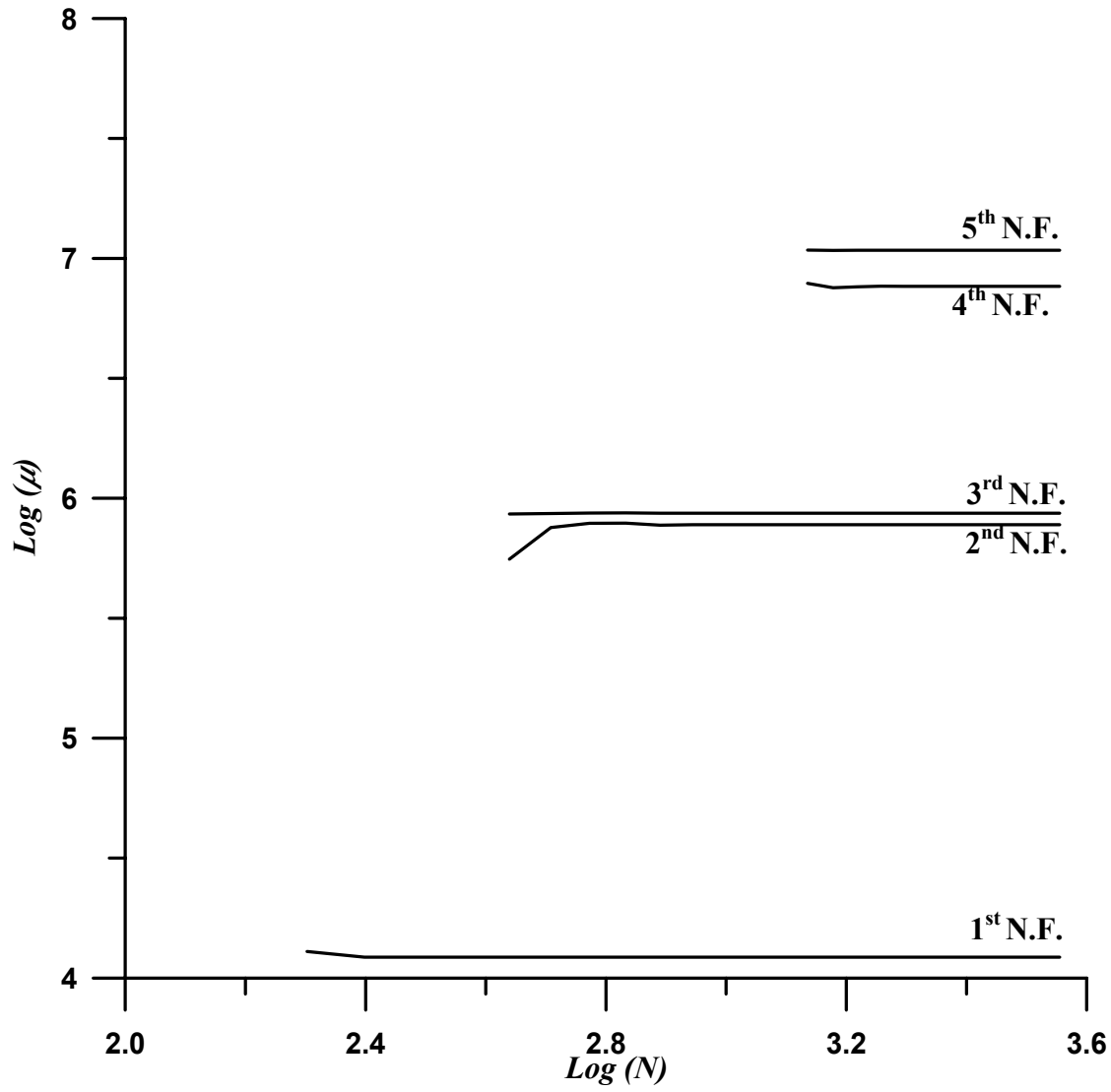


Figure 5. Convergence of the First Five Natural Frequencies

Table 1. Ordering Scheme for Bending-Torsion Coupled Timoshenko Beam Formulation

$\frac{x}{R} = O(1)$	$\frac{w}{R} = O(\varepsilon)$
$\frac{\xi}{R} = O(\varepsilon)$	$\frac{\eta}{R} = O(\varepsilon)$
$\varphi = O(\varepsilon)$	$\psi = O(\varepsilon)$
$\frac{u_0}{R} = O(\varepsilon^2)$	$\gamma = w' - \varphi = O(\varepsilon^2)$

Table 2. Area Integrals for Potential Energy Expression

$\iint_A d\eta d\xi = A$	$\iint_A \eta^2 d\eta d\xi = I_z$	$\iint_A \xi^2 d\eta d\xi = I_y$
$\iint_A \eta d\eta d\xi = Ae$	$\iint_A (\eta^2 + \xi^2) d\eta d\xi = J$	$\iint_A \xi d\eta d\xi = \iint_A \eta \xi d\eta d\xi = 0$

Table 3. Area Integrals for Kinetic Energy Expression

$\iint_A \rho d\eta d\xi = m$	$\iint_A \rho \eta^2 d\eta d\xi = \rho I_z$	$\iint_A \rho \xi^2 d\eta d\xi = \rho I_y$
$\iint_A \rho \eta d\eta d\xi = me$	$\iint_A \rho (\eta^2 + \xi^2) d\eta d\xi = I_\alpha$	$\iint_A \rho \xi d\eta d\xi = \iint_A \rho \eta \xi d\eta d\xi = 0$

Table 4. Variation of the Natural Frequencies with the Rotational Speed

Natural Frequencies (Hertz)	Angular Speed Ω (rad/s)									
	0		5		10		15		20	
	Present	Abaqus	Present	Abaqus	Present	Abaqus	Present	Abaqus	Present	Abaqus
1.10	1.10	1.40	1.40	2.04	2.04	2.78	2.78	3.56	3.54	
6.88	6.88	7.17	7.17	7.98	7.97	9.17	9.14	10.62	10.54	
19.25	19.25	19.54	19.54	20.38	20.37	21.71	21.67	23.43	23.33	
37.68	37.69	37.98	37.98	38.87	38.84	40.29	40.22	42.19	42.00	
43.72	43.69	43.73	43.71	43.76	43.78	43.80	43.90	43.87	43.99	
62.24	62.25	62.54	62.55	63.46	63.43	64.94	64.86	66.96	66.77	

Table 6. Effect of the Timoshenko Parameters and Bending-Torsion Coupling

Freuency order	Natural Frequencies (Hz)		
	Coupled Timoshenko	Uncoupled Timoshenko	Coupled Euler
1	3.55654	3.55714	3.55673
2	10.6161	10.6184	10.6183
3	23.4306	23.4395	23.4433
4	42.1918	42.2331	42.2365
5	43.8682	42.7305	43.8715
6	66.9587	67.0171	67.0791

Table 7. Effect of the Coriolis Terms

		Ω (rad/sec)							
		100		400		700		1000	
		Coriolis Included	Coriolis Discarded						
Natural Frequencies		61.9299	61.9279	90.9346	90.9643	133.168	133.272	178.593	178.85
		363.03	363.119	380.513	379.014	393.012	391.047	409.646	406.691
		379.711	379.628	398.712	400.106	458.551	460.138	539.04	541.102
		977.367	977.379	1009.02	1008.78	1074.16	1073.07	1162.7	1158.69
		1135.53	1135.52	1149.03	1149.24	1178.59	1179.59	1226.06	1229.86
		1801.82	1801.85	1832.86	1832.41	1896.51	1894.91	1983.07	1979.6

LIST of FIGURES

Figure 1. Configuration of A Uniform, Rotating, Cantilever Timoshenko Beam Featuring Bending-Torsion Coupling

Figure 2. The Cross-Sectional View and Dimensions the Uniform Timoshenko Beam with One Symmetry Axis

Figure 3. (a) Cross-Sectional View **(b)** Side View of the Bending-Torsion Deflections of The Reference Point

Figure 4. The Normal Mode Shapes of the Rotating Coupled Timoshenko Beam

Figure 5. Convergence of the First Five Natural Frequencies

LIST of TABLES

Table 1. Ordering Scheme for Bending-Torsion Coupled Timoshenko Beam Formulation

Table 2. Area Integrals for Potential Energy Expression

Table 3. Area Integrals for Kinetic Energy Expression

Table 4. Variation of the natural frequencies with the rotational speed

Table 5. Comparison with the Studies in Open Literature

Table 6. Effect of the Timoshenko Parameters and Bending-Torsion Coupling

Table 7. Effect of the Coriolis Terms